



Title	Resonance ultrasound spectroscopy for measuring elastic constants of thin films
Author(s)	Nakamura, Nobutomo; Ogi, Hirotsugu; Hirao, Masahiko
Citation	Japanese Journal of Applied Physics. 2004, 43, p. 3115-3118
Version Type	AM
URL	https://hdl.handle.net/11094/84157
rights	
Note	

The University of Osaka Institutional Knowledge Archive : OUKA

<https://ir.library.osaka-u.ac.jp/>

The University of Osaka

Resonance Ultrasound Spectroscopy for Measuring Elastic Constants of Thin Films

Nobutomo NAKAMURA, Hirotugu OGI and Masahiko HIRAO

Graduate School of Engineering Science, Osaka University, 1-3 Machikaneyama, Toyonaka, Osaka 560-8531, Japan

We show an advanced technique for measuring elastic constants C_{ij} of thin films deposited on substrates. Thin films often show anisotropy between the in-plane and out-of-plane directions because of their columnar structure, residual stress, texture, and incohesive bond. Then, thin films show macroscopically transverse isotropy and have five independent C_{ij} . All the film C_{ij} affect free-vibration resonance frequencies of the film/substrate layered specimen. Therefore, measuring the resonance frequencies permits us to determine the thin-film C_{ij} with the other known parameters. In order to yield reliable C_{ij} of thin films, we have to measure the resonance frequencies with sufficient accuracy and identify vibration modes of the measured resonance frequencies. We overcome these problems by developing a tripod and using a laser-Doppler interferometer, respectively. We applied the present technique to a copper thin film. Measured C_{ij} are smaller than those of bulk and show elastic anisotropy. We attribute these features to the incohesive bond regions.

KEYWORDS: elastic constants, laser measurement, micromechanics, resonance ultrasound spectroscopy, thin films

1. Introduction

Determination of a thin film's elastic constants C_{ij} is an important issue for designing devices such as surface-acoustic-wave (SAW) devices and microelectromechanical systems (MEMS). In addition, it enables us to evaluate micro- or nano-scale defects in the film, because they highly affect the film C_{ij} through elastic softening.

Thin films often show anisotropy between the in-plane and out-of-plane directions because of their columnar structure, residual stress, texture, and incohesive bonds. Thus, their elastic constants show transverse isotropy (or hexagonal symmetry) and have five independent elastic constants. They are denoted by C_{11} , C_{33} , C_{13} , C_{44} , and C_{66} when the x_3 axis is along the out-of-plane direction and the x_1 and x_2 axes lie in the in-plane direction. Many previous studies assumed that thin films are elastically isotropic and reported only the in-plane Young's modulus E_1 using the static bending test¹⁾ and flexural vibration of a reed composed of a film/substrate layered plate.²⁾ These methods always involve ambiguity caused by the mechanical contacts used to grip the specimen and to make the acoustic transduction. The Brillouin-scattering technique³⁾ can deduce all the five elastic constants, but failed to detect the elastic anisotropy because it is insensitive to non-Rayleigh-wave acoustic modes.

In this study, we propose an acoustic method for determining thin film C_{ij} , which is a combination of resonance ultrasound spectroscopy (RUS)^{4,5)} and laser-Doppler interferometry. The RUS method deduces thin film C_{ij} from free-vibration resonance frequencies of a film/substrate layered specimen. Mode identification for the measured resonance frequencies is indispensable for successful determination. However, few studies achieved correct mode identification. Here, we use laser-Doppler interferometry to measure the displacement distributions on the specimen surface and to identify the vibration modes.

We applied the present method to a copper thin film deposited on monocrystal silicon. Measured C_{ij} are smaller than those of bulk copper and show elastic anisotropy ($C_{11} > C_{33}$). As the cause, we consider

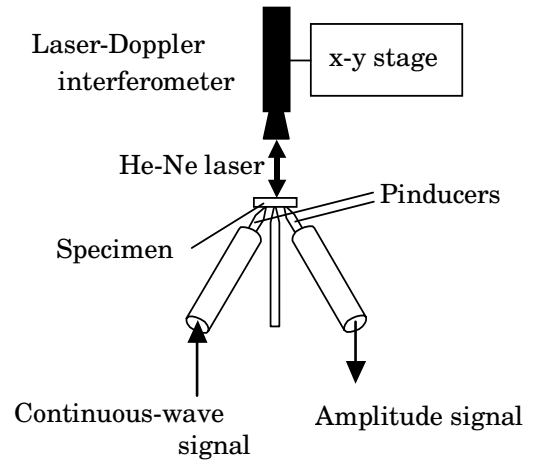


Fig. 1. Schematic of the RUS/laser measurement setup.

the effect of texture or incohesive bonds. From the X-ray-diffraction measurement and micromechanics calculation, we concluded that the presence of the incohesive bonds is the principal cause.

2. RUS/Laser Technique

Free-vibration resonance frequencies of a rectangular parallelepiped specimen depend on dimensions, mass density, and all independent elastic constants. The elastic constants are inversely determined by measuring the free-vibration resonance frequencies, dimensions, and density. This method is called RUS. Similarly, for a film/substrate layered specimen, the film C_{ij} is determined from the free-vibration resonance frequencies and dimensions, mass densities, and C_{ij} of the substrate. However, because the film C_{ij} contributes weakly to the resonance frequencies, normally as small as 1%, we must measure the resonance frequencies with a high accuracy. Previous RUS studies^{4,5)} measured the resonance frequencies by sandwiching specimens between two transducers. This setup constrains the specimen's deformation and changes the resonance frequencies from those of ideal free vibration. In order to minimize this influence,

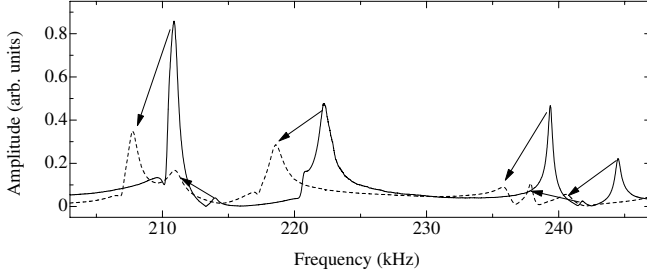


Fig. 2. RUS spectra of the monocrystal silicon substrate ($12 \times 10 \times 0.2$ mm³) (solid line) and copper ($2.3 \mu\text{m}$)/silicon layered specimen (dashed line).

we developed a piezoelectric tripod,⁶⁻⁸⁾ which consists of two piezoelectric needle-type transducers and a support needle as shown in Fig. 1. One needle-type transducer generates a sinusoidal continuous-wave (cw) vibration in the specimen and the other needle-type transducer detects the amplitude response. By sweeping the driving frequency and obtaining the amplitude as a function of the frequency, we obtain a resonance spectrum as shown in Fig. 2. The resonance frequencies are determined by fitting a Lorentzian function around the peaks. Contacts between the specimen and needle-type transducers are weak and stable because no coupling material is needed: only the specimen mass contributes to the acoustic coupling. Thus, the reproducibility of a resonance-frequency measurement is better than 10^{-4} .

The inverse calculation requires calculation of the resonance frequencies of a solid specimen. For a non-layered rectangular parallelepiped specimen, we consider minimization of the Lagrangian:

$$\delta \int_V L dV = 0 \quad (1)$$

where

$$L = \frac{1}{2} (C_{ij} S_i S_j - \rho \omega^2 u_i u_i) \quad (2)$$

denotes Lagrangian. The integration is taken over the volume V of the solid. ρ denotes the mass density, ω the angular frequency, u_i the displacement in the x_i axis, and S_i the engineering strain. Because no analytical solution exists for the displacements in a rectangular-parallelepiped solid subjected to a free vibration, the displacements are approximated by linear combinations of basis functions Ψ_k :

$$u_i(x_1, x_2, x_3, t) = \sum_k U_k^i \Psi_k^i(x_1, x_2, x_3) e^{j\omega t} \quad (3)$$

Here, U_k^i denote the expansion coefficients.

For a layered parallelepiped specimen, the formulation must include the discontinuous displacement gradients at the film/substrate interface, arising from their different moduli. Then, Heyliger⁹⁾ used different basis functions for the thickness direction (x_3) and in-plane direction (x_1 and x_2) as

$$\Psi_k^i(x_1, x_2, x_3) = \eta_m^i(x_3) \zeta_l^i(x_1, x_2), \quad (4)$$

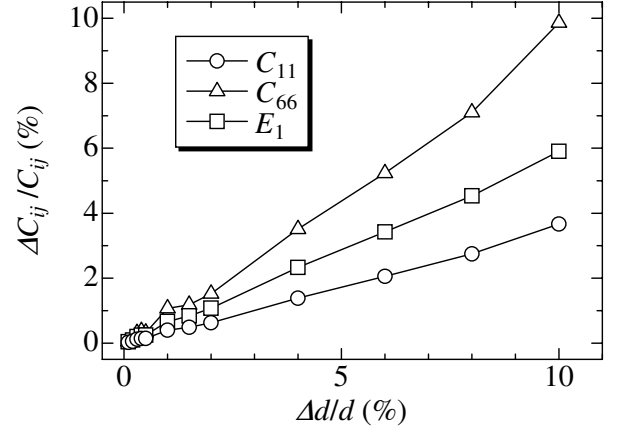


Fig. 3. Relationship between the film thickness error and errors in the resultant film C_{ij} .

where $\eta_m^i(x_3)$ denotes the one-dimensional Lagrangian interpolation polynomials and $\zeta_l^i(x_1, x_2)$ denotes power series $x_1^p x_2^q$ ($p, q = 0, 1, 2, \dots$). Substituting eqs. (3) and (4) into eq. (1) results in the matrix form of

$$\omega^2 [\mathbf{M}] \{\mathbf{U}\} = [\mathbf{K}] \{\mathbf{U}\}. \quad (5)$$

Here, $[\mathbf{M}]$ denotes the mass matrix associated with the kinetic energy of the system and $[\mathbf{K}]$ denotes the stiffness matrix associated with the potential energy of the system. $\{\mathbf{U}\}$ denotes the eigenvector composed of the expansion coefficients, which provide the displacement distributions in the specimen with eq. (3). Thus, the analysis is formulated in an eigenvalue problem and the resonance frequencies are obtained from the eigenvalues of the system. The thin film elastic constants are inversely determined by comparing the calculated resonance frequencies with the measurements. We used a standard least-squares-fitting procedure in Heyliger's method to determine a set of elastic constants that minimizes the differences between measured and calculated resonance frequencies. Such a calculation method was confirmed by Ogi *et al.*¹⁰⁾

To determine the film C_{ij} inversely from the resonance frequencies, correct correspondence of the observed and calculated resonance frequencies must be achieved. If the inverse calculation contains mode misidentification, the resulting C_{ij} are physically meaningless. However, the mode identification has never been straightforward, because the resonance spectrum does not include any information on modes. We overcome this by mapping the out-of-plane displacements using a laser-Doppler interferometer (Fig. 1) and comparing them with the calculated displacement distributions.

3. Measurement Accuracy

There are two possible error sources in the determined film C_{ij} : (i) measurement error of the film thickness and, (ii) measurement error of the resonance frequencies. Here, we investigate their influences on the determined film C_{ij} .

Table I. Measured and calculated elastic constants (GPa) of copper thin film deposited on a 0.2-mm monocrystal silicon substrate. $C_{66} = (C_{11} - C_{12})/2$.

	Copper thin film (2.3 μm)	Hill averaging (isotropic)	Micromechanics (porosity= 6.2×10^{-4})	(111) texture
C_{11}	172.6 ± 13.8	197.7	169.7	213.3
C_{33}	92.0 ± 7.0	197.7	94.8	237.9
C_{13}	134.0 ± 5.1	103.0	49.4	87.1
C_{12}	80.7 ± 15.1	103.0	75.0	111.7
C_{44}	—	47.4	36.1	35.7
C_{66}	45.9 ± 6.1	47.4	47.3	50.8

3.1 Measurement error of dimensions

We determine the film thickness by its cross-sectional SEM observation. Because the measurement of the film thickness usually includes the largest error, we estimate its effect numerically by considering a copper/silicon layered model. The substrate is a monocrystal silicon substrate, measuring $12.000 \pm 0.000 \pm 0.200 \text{ mm}^3$ with the (100) face normal to the out-of-plane direction. Copper film is 3 μm thick. We calculated the free-vibration resonance frequencies of the layered specimen and determined the film C_{ij} assuming various film-thickness errors ($d + \Delta d$). Figure 3 shows the results. The errors in the resultant C_{ij} are in proportion to the film thickness errors. The film-thickness variation in the cross-sectional observation is approximately 5% at most, indicating that errors caused by the film-thickness error in the C_{ij} are less than 5%.

3.2 Measurement errors of resonance frequencies

The measurement errors of the resonance frequencies significantly affect the resulting film C_{ij} . We estimate this (ΔC_{ij}) from the contributions of the C_{ij} to the resonance frequencies ($\partial f / \partial C_{ij}$) and measurement errors of the resonance frequencies (Δf) as

$$\Delta C_{ij} = \frac{1}{\partial f / \partial C_{ij}} \Delta f, \quad (6)$$

$\partial f / \partial C_{ij}$ is obtainable from the inverse calculation.⁵⁾ Thus, elastic constants with smaller contribution cannot be determined accurately.

4. Elastic Constants of Copper Thin Film

We applied the present method to a polycrystalline copper film deposited on a monocrystal silicon substrate ($12.019 \pm 0.009 \pm 0.211 \text{ mm}^3$). First, we measured the resonance frequencies of the substrate alone to determine the substrate C_{ij} . They agreed with well known values¹¹⁾ within a 1% difference. Then, we deposited the copper film by the magnetron-sputtering method and measured the resonance frequencies of the Cu/Si specimen. The pressure in the sputtering chamber was kept less than 5×10^{-5} Torr prior to the sputtering; it increased up to 0.05 Torr during the sputtering because of the addition of high-purity argon gas. The biasing voltage was 400 V and the current was 200 mA. The deposition rate was 3 $\text{\AA}/\text{s}$. The film thickness was 2.3 μm and the X-ray diffraction spectrum indicates a (111) texture. We calculated the lattice parameter of the copper thin film from the X-ray diffraction spectrum, which agreed with the bulk's value with a difference of 0.1%. Also, SEM

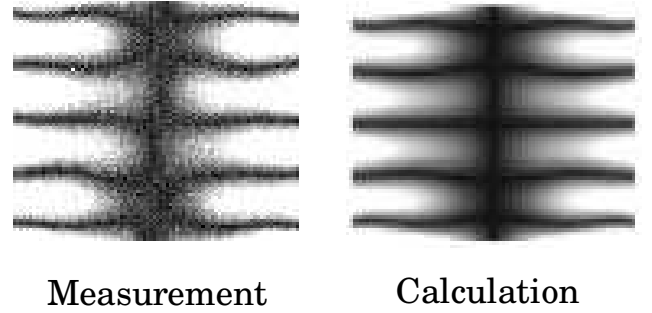


Fig. 4. Measured (left) and calculated (right) displacement-amplitude distributions of 2.3- μm -thick copper/0.2-mm silicon vibrating at 151.4 kHz.

observation did not reveal any volume defects. Therefore, we used the mass density of bulk copper for the film. After the deposition, the resonance peaks shifted to lower frequencies as shown in Fig. 2. Figure 4 shows an example of the comparison between the measured and computed displacement distributions for the Cu/Si specimen. We see excellent agreement between them, which ensures correct mode identification. Thus, we identified more than twenty resonance modes and entered them into the inverse calculation to determine the film C_{ij} .

Table I shows the determined copper thin film C_{ij} along with the isotropic C_{ij} calculated by Hill approximation using monocrystal data. We failed to determine the film C_{44} because of its very small contributions to the resonance frequencies. Significant observations are (1) the C_{33} is markedly smaller than C_{11} and (2) the film C_{ij} are smaller than those of the ideal isotropic C_{ij} . As a possible cause of this anisotropy, we consider (i) texture and (ii) local incohesive bonds. The observed X-ray-diffraction spectrum indicates the (111) planes oriented preferentially parallel to the film surface. We calculated the macroscopic C_{ij} of such a textured microstructure in which all the (111) planes of grains are aligned parallel to the x_3 surface with a random rotation around the x_3 axis. The Hill approximation was used for this calculation. The calculated C_{ij} values appear in Table I. The C_{33} of the copper film is larger than C_{11} in the case of the (111) texture; this result is opposite to the observed results. Thus, the texture cannot be a dominant factor of the observed anisotropy.

Second, we consider the presence of incohesive bonds at grain boundaries by micromechanics modeling. For

copper thin films, Schwaiger *et al.*¹²⁾ reported that thinner films are more fatigue-resistant and contain fewer and smaller extrusions than thicker films. They attributed this observation to vacancy diffusion and annihilation at the free surface. We assumed that there are incohesive regions parallel to the in-plane direction and estimate their effect by replacing them with penny shaped microcracks. The elastic constants of such a two-phased composite (C_c) are calculated using Eshelby's equivalent inclusion theory¹³⁾ and Mori-Tanaka's mean field theory¹⁴⁾ as

$$\begin{aligned} \mathbf{C}_c &= \mathbf{C}_M + [f_I (\mathbf{C}_I - \mathbf{C}_M) \mathbf{A}_d] [f_M \mathbf{I} + f_I \mathbf{A}_d]^{-1}, \\ \mathbf{A}_d &= [\mathbf{S} \mathbf{C}_M^{-1} (\mathbf{C}_I - \mathbf{C}_M) + \mathbf{I}]^{-1} \end{aligned} \quad (7)$$

where \mathbf{C}_M and \mathbf{C}_I are elastic-constant tensors of the matrix and inclusions, respectively, and \mathbf{S} is Eshelby's tensor. f_M , and f_I are volume fractions of the matrix and inclusion. Eshelby's tensor depends on the shape of the inclusion and Poisson's ratio of the isotropic matrix. We assumed zero modulus and $a_1:a_2:a_3=1:1:0.001$ for the inclusions (a_i are axes of the oblate-ellipsoid inclusions). When the porosity is 6.2×10^{-4} , the calculation gives the diagonal components of the elastic constants close to those of the measurements as shown in Table I. Thus, only the incohesive regions can explain the occurrence of the C_{33} smaller than C_{11} and smaller C_{ij} than those of the bulk material.

5. Conclusion

In this study, we established the RUS/laser measurement for the thin film C_{ij} and determined the anisotropic elastic constants of 2.3 μm copper film. The elastic constants of the copper film show anisotropy between the in-plane and out-of-plane directions. We conclude that the incohesive bonds caused this anisotropy.

- 1) A. Rouzaud, E. Barbier, J. Ernoul and E. Quesnel: *Thin Solid Films* **270** (1995) 270.
- 2) S. Sakai, H. Tanimoto and H. Mizubayashi: *Acta Mater.* **47** (1999) 211.
- 3) P. Djemia, F. Ganot, P. Moch, V. Branger and P. Goudeau: *J. Appl. Phys.* **90** (2001) 756.
- 4) I. Ohno: *J. Phys. Earth* **24** (1976) 355.
- 5) A. Migliori, J.L. Sarrao, W.M. Visscher, T.M. Bell, M. Lei, A. Fisk and R.G. Leisure: *Physica B* **183** (1993) 1.
- 6) H. Ogi, Y. Kawasaki, M. Hirao and H. Ledbetter: *J. Appl. Phys.* **92** (2002) 2451.
- 7) N. Nakamura, H. Ogi, T. Ichitsubo, M. Hirao, N. Tatsumi, T. Imai and H. Nakahata: *J. Appl. Phys.* **94** (2003) 6405.
- 8) N. Nakamura, H. Ogi and M. Hirao: *Acta Mater.* **52** (2004) 765.
- 9) P. Heyliger: *J. Acoust. Soc. Am.* **107** (2000) 1235.
- 10) H. Ogi, P. Heyliger, H. Ledbetter and S. Kim: *J. Acoust. Soc. Am.* **108** (2000) 2829.
- 11) G. Simmons and H. Wang: *Single Crystal Elastic Constants and Calculated Aggregate Properties : a Handbook* (The M.I.T. PRESS, Cambridge, 1971).
- 12) R. Schwaiger, G. Dehm and O. Kraft: *Philos. Mag.* **83** (2003) 693.
- 13) J.D. Eshelby: *Proc. Roy. Soc. London*, **A241** (1957) 376.
- 14) T. Mori and K. Tanaka: *Acta Metall.* **21** (1973) 571.